Bioorganic & Medicinal Chemistry 20 (2012) 628–632

Contents lists available at ScienceDirect

Bioorganic & Medicinal Chemistry

journal homepage: www.elsevier.com/locate/bmc

Activity based subcellular resolution imaging of lipases

Martin Viertler [†], Matthias Schittmayer [†], Ruth Birner-Gruenberger [*]

Proteomics Core Facility, Center for Medical Research and Institute of Pathology, Medical University of Graz, Stiftingtalstrasse 24, A-8010 Graz, Austria

ARTICLE INFO

Article history:
Available online 19 April 2011

Keywords:
Activity based proteomics
On-slide click chemistry
Activity based cell imaging
Subcellular lipase localization

ABSTRACT

Lipases play a key role in whole body energy homeostasis. Dysregulation of lipolytic activities affects lipid absorption, mobilization, and transport, and is causative for lipid-related diseases. Regulation of enzymes involved in lipid metabolism is governed by a complex network of protein–protein and protein–small molecule interactions. Thus these enzymes have to be studied under the physiologically most relevant conditions, that is, in vivo. Our latest generation of activity based probes designed for capturing of lipases employs bioorthogonal chemical linker groups, which are membrane permeable and thus allow studying protein activity in living cells. Another advantage is the virtually unlimited choice of reporter tags. Here we report on a novel method combining in vivo activity based labeling of lipases with in situ detection of lipolytic activities by on slide click chemistry and imaging by fluorescence microscopy. We demonstrate that cytosolic as well as organelle resident lipases are specifically labeled in intact living cells. This method will shed light on the (sub)cellular localization of lipolytic proteomes of cells and tissues in health and disease directly at enzymatic activity level without the need of prior knowledge of the identities of the responsible enzymes or dependence on the availability of specific antibodies.

1. Introduction

Lipases are key players in whole body energy homeostasis.[1] Control of lipolysis of triacylglycerols and cholesteryl esters stored in lipid droplets of adipose tissue plays an important role in energy partitioning and balance and maintains the size of fat depots in the body. Dysregulation of these lipolytic activities affects lipid absorption, mobilization and transport, and is causative for lipid-related diseases. As many enzymes, lipases are strongly regulated at the posttranslational level.

Activity based probes (ABP) are ideal tools to observe changes in enzyme activities, providing a readout of enzymatic activity rather than mere protein abundance. These probes typically consist of a reactive group, a binding group and a reporter tag. While the reactive group covalently binds the probe to the target protein based on the target's enzymatic mechanism, the binding group ensures the probe is recognized by the target protein as a potential substrate in the first place. The reporter tag can either be an affinity tag,[2] a fluorophore,[2,3] or, in the latest generation of ABP, a so called bioorthogonal linker group.[4,5] These groups are small and biologically inert yet they can be targeted with high specificity in a subsequent step, for example by a click chemistry reaction. Major advantages of this approach are the superior membrane permeability of the probes and no adverse effect of the reporter tag on probe recognition, both frequently observed for fluorophore carrying ABP.[6] One possibility to couple the bioorthogonal linker group and the reporter tag is copper catalyzed azide alkyne [3+2] cycloaddition (CuAAC).[7] In recent years several click chemistry reactions, including Staudinger ligation,[8] strain promoted azide alkyne cycloaddition[9,10] and CuAAC[11] have been successfully employed to visualize small molecules[8,10,12–14] as well as proteins[15,16] in metabolic labeling experiments.

While the lower abundance of proteins as compared to many small molecules used for metabolic labeling is an issue, several possible solutions for this problem have been established. First, the intrinsic signal amplification capability of enzymes can be exploited by using fluorogenic substrates to visualize enzymatic activity.[17,18] However, the released fluorescent products are often soluble and limit spatial resolution to the cellular level, with cell membranes acting as natural diffusion barrier. Another approach by Blum et al.[19] relied on reducing background by designing an ABP carrying quenchers next to the fluorescent tag, which were released upon binding to the target enzymes. This approach was successfully used for whole body imaging of mice.[20] Recently, Yang et al.[21] employed alkyne modified versions of the antiobesity drug Orlistat to identify potential side targets of the drug and also tested the applicability of these probes for imaging applications. While

Abbreviations: ABP, activity based probe; ACN, acetonitrile; ATGL, adipose triglyceride lipase; CuAAC, copper (I) catalyzed azide alkyne [3+2] cycloaddition; DIPEA, diisopropylethylamine; FA, formic acid; HSL, hormone sensitive lipase; MGL, monoglyceride lipase; TGH1, triacylglycerol hydrolase.

* Corresponding author. Tel.: +43 31638572962; fax: +43 31638573009.
E-mail address: ruth.birner-gruenberger@medunigraz.at (R. Birner-Gruenberger).

† These authors contributed equally to the study and should therefore be regarded as co-first authors.

0968-0896/$ - see front matter © 2011 Elsevier Ltd. All rights reserved.
doi:10.1016/j.bmc.2011.04.018

they succeeded to label the major Orlistat target, namely fatty acid synthase, as well as several other proteins in gel based experiments, fluorescence microscopy experiments showed an ER localized activity based stain, in contrast to the cytosolic stain observed for immuno-histochemical detection of fatty acid synthase.

Here we report the application of activity based click probes for in vivo labeling of lipases with on slide click chemistry and confocal fluorescence microscopy to realize in situ visualization of lipolytic activities in the cell (Fig. 1). Since one of the major mechanisms regulating lipolytic activity is localization of lipases to or from lipid droplets, we followed published fixation procedures optimized to ensure lipid droplet structural integrity.[22] Moreover, we established a quadruple staining method to allow staining of nuclei and lipid droplets, as well as protein immunodetection next to activity based labeling of the lipolytic activities.

Proteins tagged included the known intracellular lipases involved in mobilization of intracellular triacylglycerols from lipid droplets, namely adipose triglyceride lipase (ATGL),[23] hormone sensitive lipase (HSL)[24] and monoglyceride lipase (MGL),[25] as well as the ER luminal triacylglycerol hydrolase 1 (TGH1).[26]

2. Material and methods

If not stated otherwise, reagents were purchased from Sigma–Aldrich, Vienna, Austria.

2.1. Cell culture

All cell culture reagents were purchased from PAA laboratories, Pasching, Austria. African green monkey kidney cells (COS-7; ATCC Number CRL-1651) were propagated in full media (Dulbecco's Modified Eagle's Medium (DMEM); 10% fetal bovine serum; penicillin/streptomycin) at 37 °C in a humidified atmosphere, 5% CO_2.

2.2. Transfection

N-Terminal HIS-tag fusion constructs of beta-galactosidase (LacZ), murine hormone sensitive lipase (HSL), adipose triglyceride lipase (ATGL) and monoglyceride lipase (MGL)[27,28] as well as the N-terminal GFP fusion construct of MGL[29] were kindly provided by Rudolf Zechner, University of Graz, Austria. The TGH1-eGFP[30] fusion construct used in this study was a kind gift of Richard Lehner, University of Alberta, Canada. 5×10^4 COS-7 cells were seeded on chamber slides (BD Biosciences, Vienna, Austria) the day before transfection. Turbofectene™ in vitro reagent (Fermentas, St. Leon-Rot, Germany) was used to transfect 0.5 μg of plasmid DNA per chamber according to the manufacturers instructions. Stains were performed 48 h post transfection. HIS-MGL and GFP-MGL transfected cells were loaded overnight with 150 μM oleic acid complexed to fatty acid free bovine serum albumin (PAA laboratories, Pasching, Austria) in a 3:1 molar ratio, as indicated in the text. For 4-nitrophenyl butyrate hydrolase assays, transfection was performed with 6 μg DNA in 25 cm^2 cell culture flasks.

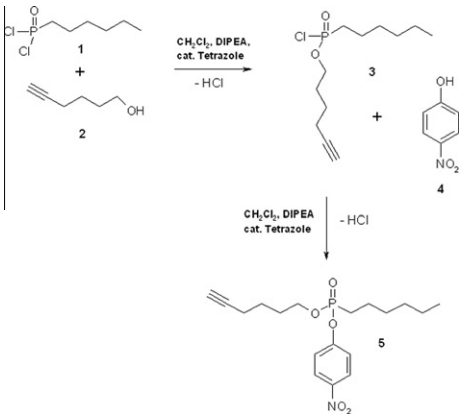

Scheme 1. Synthesis of activity based click probe. 5-hexyn-1-ol diluted (**2**) was added drop-wise to hexylphosphonic acid dichloride (**1**). Subsequently, intermediate product (**3**) was reacted with 4-nitrophenyl (**4**) to yield hexynyl-4-nitrophenyl-hexylphosphonate (**5**).

2.3. Synthesis of activity based click probe hexynyl-4-nitrophenyl-hexylphosphonate (5) (Scheme 1)

Two millimolars of hexylphosphonic acid dichloride (**1**) was dissolved in a mixture of 5 mL absolute CH_2Cl_2, 10 mmol diisopropylethylamine (DIPEA) and 0.2 mmol tetrazole (0.45 M in acetonitrile (ACN)). Two millimolars of 5-hexyn-1-ol diluted (**2**) in 20 mL absolute CH_2Cl_2 was added drop-wise to the stirred solution. After complete addition, the resulting mixture was stirred another 4 h at room temperature. Reaction was monitored by TLC. After completion, 5 mmol 4-nitrophenyl (**4**) and 5 mmol DIPEA was added to the product (**3**), the reaction was stirred for 16 h at room temperature. Reaction was monitored by TLC and after completion product (**5**) was confirmed by LC–MS (reverse phase C18; H_2O/ACN + 0.1% formic acid (FA); linear gradient from 0 min 40% ACN to 10 min 100% ACN, positive full scan MS m/z 150–1000). All volatile components were removed under reduced pressure on the rotary evaporator. The residue was dissolved in 10 mL CH_2Cl_2 and washed twice with 1 M aqueous K_2CO_3 (20 mL), twice with water (20 mL) and once with brine (20 mL) before drying over sodium sulfate. Sodium sulfate was removed by filtration and volatiles were removed under reduced pressure on the rotary evaporator. Residue was dissolved in 5 mL of H_2O/ACN (60:40) and purified by HPLC (reverse phase C18; H_2O/ACN + 0.1% FA; linear gradient

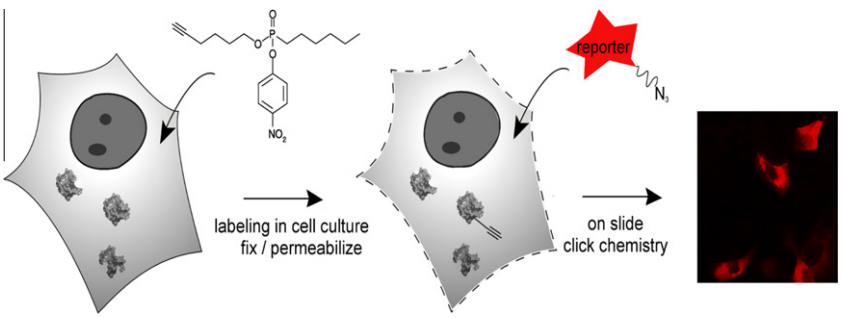

Figure 1. Workflow for activity based imaging of lipases. A schematic overview on the procedure is given. First activity based labeling of lipases is achieved in living cells. Before click chemistry is applied on the specimen, the cells are fixed and permeabilized to achieve efficient translocation of click components into the cells.

from 0 min 40% ACN to 10 min 100% ACN). Fractions containing the click probe were dried and the probe was subjected to LC–MS and NMR analysis. m/z = 368.3 (expected $[M+H]^+$ = 368.4); ^1H NMR ($CDCl_3$): δ 8.23 (m, 2H), 7.35 (apparent d, 2H), 4.13 (t, 2H, J = 8 Hz), 2.20 (m, 1H), 2.10 (apparent s, 4H), 1.95–2.04 (m, 2H), 1.39–1.83 (m, 4H), 1.26 (apparent t, 6H), 0.87 (t, 3H, J = 7 Hz). ^{13}C NMR ($CDCl_3$): δ 155.3, 141.3, 126.5, 126.1, 121.4, 83.6, 69.4, 61.1, 31.4, 30.3, 29.5, 24.6, 22.5, 22.3, 21.4, 18.1, 14.3, 14.2.

2.4. Labeling of cells in culture

Stocks of click probe were dissolved in dichloromethane, divided into aliquots of 30 or 100 nmol, dried in vacuo and stored at −20 °C until use. Full media within chambers was exchanged twice for phosphate buffered saline (PBS) to remove serum components 48 h after transfection. Dried probe aliquots were taken up in 10 μl DMSO and added to 1 mL DMEM containing Penicillin/Streptomycin to a final concentration of 30 or 100 μM (as indicated in the text). Next PBS was exchanged for the labeling mix and cells were incubated for 2 h (37 °C; humidified atmosphere; 5% CO_2). Efficiency of labeling was assessed by subjecting cell lysates to 4-nitrophenyl butyrate esterase activity assays as described by Lehner and Verger.[31]

2.5. In situ detection of lipases

Fixation was performed as described by DiDonato et al.[22] with 3% formaldehyde in PBS for 10 min at room temperature. Following fixation, cells were rinsed three times by incubation in PBS for 5 min in total.

For HIS-tagged lipases, the cells were blocked and permeabilized in blocking buffer (PBS containing 1% fatty acid free bovine serum albumin (PAA laboratories, Pasching, Austria) and 0.1% Tween 20 (Bio-Rad Laboratories, Vienna, Austria)) for 30 min at room temperature. Next, a mouse anti HIS-Dylight647 antibody (Tebu-bio, Offenbach, Germany) diluted to 2 μg/mL in blocking buffer was incubated for 1 h at room temperature. CuAAC was performed using 0.1 mM tris-(benzyltriazolylmethyl)amine (TBTA)[32] ligand, 5 mM copper(II)sulfate, 10 mM sodium ascorbate and 50 μM Atto532-azide (Atto-Tec, Siegen Germany). Nuclei were counterstained for 10 min with Hoechst 33422 (0.1 μg/mL in PBS). Lipid droplets were counterstained with BODIPY 495/505 (Invitrogen, Vienna, Austria) (0.2 μg/mL in PBS) for 10 min.

For indirect labeling of GFP-MGL, the cells were permeabilized with PBS containing 1% bovine serum albumin and 0.1% saponin or 0.1% Tween 20 for 10 min. CuAAC coupling of biotin–azide (Invitrogen, Vienna, Austria) to alkyne modified lipases was performed using 0.5 mM bathocuproinsulfonate (BCS) as ligand, 2 mM copper(II)sulfate, 15 mM sodium ascorbate and 50 μM biotin–azide (in 100 mM Tris–HCl, pH 8). CuAAC was performed for 2 h at 37 °C. Next, the slides were incubated with streptavidin–Atto532 conjugate in blocking buffer for 1 h at room temperature.

For direct labeling of TGH-eGFP CuAAC reaction contained 0.5 mM BCS, 2 mM copper(II)sulfate, 15 mM sodium ascorbate and 50 μM Atto532-azide and proceeded for 1 h at 37 °C. Cells were counterstained with 0.1 μg/mL Hoechst 33342 in PBS. In between all labeling steps, the slides were washed three times in PBS for 5–10 min in total. In all experiments slides were mounted in fluorescence mounting media (Dako, Vienna, Austria). Images were acquired on a LSM510 Meta confocal laser scanning microscope (Zeiss, Oberkochen, Germany) using a 63× oil immersion objective (NA 1.4). The following excitation laser wavelengths/emission filter settings were used: 488 nm/505–530 nm band pass (GFP, YFP, BODIPY); 543 nm/560–615 nm band pass (Atto532-azide, Atto532–streptavidin, Rho6G-azide); 633/650 nm long pass (HiLyte Fluor647, Atto647-azide). Image acquisition for activity based stains, Dylight647/GFP signals and counterstains were performed in separate acquisition tracks. Montages of images were prepared in ImageJ[33] and contrast and brightness were adjusted.

3. Results

3.1. Labeling with activity based probe

We transiently expressed the major cytosolic lipases (i.e., ATGL, HSL, and MGL) fused to a HIS-tag in COS-7 cells. This cell line was previously reported to show very low intrinsic lipase activity[28] and was therefore ideally suited to verify the specificity of our method.

To determine the degree of labeling of the ABP, we employed a 4-nitrophenyl butyrate hydrolase assay.[31] Cells expressing HIS-MGL incubated for 2 h with serum free media containing 30 μM click probe showed no detectable residual lipolytic activity, indicating a quantitative inhibition of lipases, while a control reaction without probe showed an activity of 37 nmol min^{-1} mg^{-1} cell lysate (Supplementary Fig. 1).

3.2. Activity based imaging of lipases

COS-7 cells expressing HIS-tagged versions of ATGL, HSL, and MGL were incubated with activity based click probe in culture. After cell fixation Atto532-azide was coupled to the probe by CuAAC. We were able to observe a clear cytosolic signal (Fig. 2, panels A) corresponding to successfully transfected cells as controlled by an anti-HIS antibody stain (Fig. 2, panels B). Moreover, the expression patterns within the cell showed an almost perfect overlap of the two complementary stains (Fig. 2, panels C). To rule out background staining caused by either activity based probe or subsequent CuAAC, COS-7 cells expressing a HIS-LacZ fusion constructs were used as a mock control. In this case, only a low background signal was observed and it did not correlate to HIS-LacZ expression (Fig. 2).

We also observed that non lipid loaded COS-7 cells only exhibited little to no lipid droplets, as shown by a BODIPY495/505 counterstain (Fig. 2 C, white). Accordingly, the general appearance of HIS-tagged lipases in COS-7 cells lacked lipid droplet like structures. Therefore, we loaded COS-7 cells expressing HIS-MGL with oleic acid. As expected, a BODIPY 495/505 stain resulted in lipid droplet like structures, but no accumulation of fluorescent signal in the vicinity of these structures was observed for either activity based or antibody stain.

While the spatial overlap of the activity based and antibody stains was very good from the start, one of our major concerns was variation of the intracellular signal intensities between the two stains (non-uniform color distribution of overlays, Fig. 2, panels C). We speculated that these intensity differences might be caused by partial incompatibility of the immuno-histochemical detection with the CuAAC and therefore switched our experimental set up to GFP-tagged lipases.

Indeed, the activity based stain of COS-7 cells expressing YFP-ATGL and GFP-MGL, respectively, did not only match the spatial distribution of the GFP-signal but the two signals also exhibited a highly uniform intensity distribution (Fig. 3A–C, Supplementary Fig. 2). Interestingly, while we were unable to observe preferred localization to lipid droplet like structures in oleate loaded cells for HIS-tagged lipases, the GFP-tagged counterparts showed a clearly increased signal intensity encircling these structures for the activity based stain as well as the GFP-signal. A negative control CuAAC with unlabeled cells resulted in very low unspecific background labeling (Supplementary Fig. 3).

As biotin–streptavidin recognition serves as platform for a variety of signal amplification strategies in light and fluorescence microscopy, we also tested the compatibility of our method to

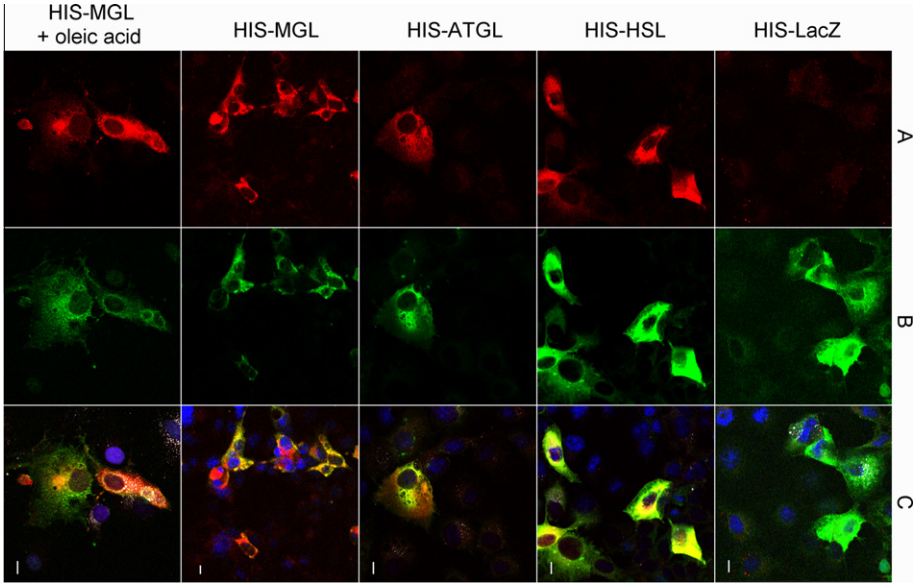

Figure 2. The activity based click probe detects cytosolic lipases in intact cells. COS-7 cells over-expressing HIS fusion constructs LacZ, HSL, ATGL, and MGL were labeled by activity based probe (A) and by a Dylight647 coupled anti HIS antibody (B). As expected, all lipases were detected by the activity based click probe, while no specific interaction of the probe with LacZ negative control was observed. In C, counterstains for nuclei (Hoechst 34422, blue false color) and lipid droplets (BODPIY 495/505, white) are provided in an overlay. Only few endogenous lipid droplets were observed; to prove the feasibility of lipid droplet co-localization in our method MGL-HIS expressing cells were loaded with oleic acid; scale-bars: 10 μm.

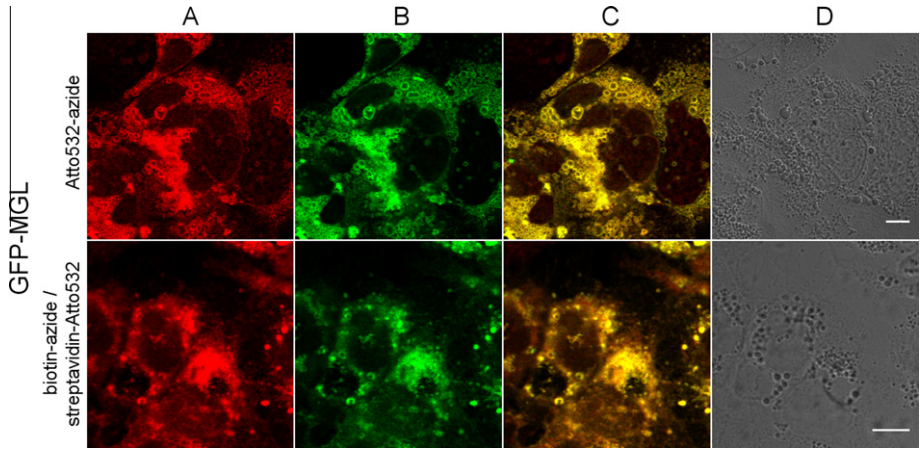

Figure 3. The GFP-MGL fusion construct is detected by both direct and indirect labeling methods. COS-7 cells over-expressing GFP-MGL[29] (B) were labeled for lipase activity as described in Sections 2.4 and 2.5; BCS was used as Cu(I) ligand. Activity based click probe GFP-MGL was either detected directly with Atto532-azide (A, upper panel), or indirectly by biotin–azide coupling and subsequent streptavidin–Atto532 recognition (A, lower panel). Both detection methods correlate to the GFP-MGL (see overlay in C) signal. In D a transmission image is provided to depict cell boundaries. In contrast to the HIS-MGL construct, localization patterns indicative of lipid droplets were readily observed; scale-bar: 10 μm; *z*-plane thickness: <1 μm.

biotin–streptavidin coupling. As depicted in Fig. 3, biotin labeled GFP-MGL was readily detected employing a streptavidin–Atto532 conjugate after CuAAC.

After demonstrating that our ABP was able to enter intact cells by successfully staining three lipases located in the cytosol, we were interested if we would also be able to target lipases within subcellular compartments. To address this question, we employed a GFP-tagged TGH, which was reported to reside within the lumen of the ER.[26] Also in this case, we observed highly similar signal distribution for activity based stain and GFP-signal (Fig. 4).

4. Discussion

A major advantage of ABP with bioorthogonal linkers is their ability to readily diffuse across cellular membranes. Therefore, the probes can be employed to label their target enzymes within their native subcellular compartments, ensuring optimal conditions for each individual target enzyme. Moreover, membrane permeability of ABP is a major issue for in vivo applications. Surprisingly bulky and charged substrates and inhibitors have been successfully employed for in vivo experiments, especially for the visualization of proteases.[17–20] Unfortunately, the exact mechanism of cellular uptake of these compounds remains poorly understood in most cases and it is generally assumed that endocytosis plays a major role in the process.[17,18] Since the fate of triacylglycerols and cholesteryl esters undergoing endocytosis is hydrolysis by lysosomal acid lipase[34] this pathway is barred for activity based probes mimicking lipids, underlining the importance of membrane permeable ABP in this context.

Here we successfully labeled three major cytosolic lipases and one ER residing lipase with ABP in living cells. Activity assays revealed that probe concentrations as low as 30 μM were sufficient

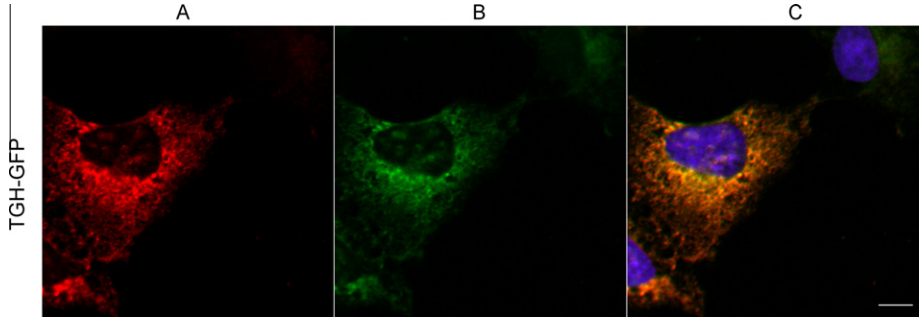

Figure 4. The activity based probe labels lipases within the ER in intact cells. An ER resident TGH-eGFP fusion construct[30] was over-expressed in COS-7 cells (B). The cells were stained for lipase activity as described in Sections 2.4 and 2.5 (A). CuAAC was performed with BCS as Cu(I) ligand. Nuclei were counterstained with Hoechst 333422 and depicted in a merge of channels (C). The activity based stain (shown in red) co-localizes with the TGH-eGFP signal (shown in green). Scale-bar: 10 μm; *z*-plane thickness: 2 μm.

to quantitatively inhibit and thereby label all tested lipases within 2 h. Subsequent fixation and coupling of fluorophores to the lipase-bound probes by CuAAC resulted in a highly specific activity based stain.

Interestingly, localization of cytosolic lipases within the cell was influenced to some extent by the choice of the N-terminal fusion partner. While GFP-tagged lipases showed an expected accumulation around lipid droplets in oleate loaded cells, HIS-tagged lipases were evenly distributed in the cytosol. Since the antibody detection matches the activity based stain, we suppose that the pattern of HIS-tagged lipases is not an artifact caused by failure of the antibody to detect lipid masked epitopes on the lipid droplet surface. Rather, the six highly polar histidine residues likely prevent accumulation in the hydrophobic environment of lipid droplets.

While the growing choice of commercially available azide modified fluorophores already allows rather complex multi-dye experiments, biotin–streptavidin interaction could further improve the choice of available fluorophores, also considering streptavidin–fluor conjugates of otherwise often highly hydrophobic far red dyes. Even more importantly, this interaction also serves as a starting point for many commercially available signal amplification systems. Essentially, the signal/noise ratio of labeled cells clicked with biotin–azide and subsequently stained with a streptavidin–Atto532 conjugate was comparable to that of direct azide–Atto532 coupling and no extensive staining of endogenous biotinylated proteins was observed.

Conclusively, we expect that this study will open up new ways for diagnostics and therapeutic intervention of lipid-related diseases by shedding light on the (sub)cellular localization of lipolytic proteomes of cells and tissues in health and disease directly at enzymatic activity level.

Acknowledgments

This work was supported by the GOLD III (Genomics of Lipid associated Disorders III; http://gold.uni-graz.at/) project in the framework of GEN-AU (Genome research in Austria; http://www.gen-au.at/) funded by the Bundesministerium für Wissenschaft und Forschung (BM.W_F).

Supplementary data

Supplementary data associated with this article can be found, in the online version, at doi:10.1016/j.bmc.2011.04.018.

References and notes

1. Schittmayer, M.; Birner-Gruenberger, R. *J. Prot.* **2009**, *72*, 1006.
2. Birner-Gruenberger, R.; Susani-Etzerodt, H.; Kollroser, M.; Rechberger, G. N.; Hermetter, A. *Proteomics* **2008**, *8*, 3645.
3. Birner-Gruenberger, R.; Susani-Etzerodt, H.; Waldhuber, M.; Riesenhuber, G.; Schmidinger, H.; Rechberger, G.; Kollroser, M.; Strauss, J. G.; Lass, A.; Zimmermann, R.; Haemmerle, G.; Zechner, R.; Hermetter, A. *Mol. Cell. Proteomics* **2005**, *4*, 1710.
4. Speers, A. E.; Cravatt, B. F. *Chem. Biol.* **2004**, *11*, 535.
5. Schicher, M.; Jesse, I.; Birner-Gruenberger, R. In *Lipidomics*; Armstrong, D., Ed.; Humana Press Inc.: New York, 2010; Vol. 2, pp 251–266.
6. Greenbaum, D.; Baruch, A.; Hayrapetian, L.; Darula, Z.; Burlingame, A.; Medzihradszky, K. F.; Bogyo, M. *Mol. Cell. Proteomics* **2002**, 60.
7. Kolb, H. C.; Finn, M. G.; Sharpless, K. B. *Angew. Chem., Int. Ed.* **2001**, *40*, 2004.
8. Saxon, E.; Bertozzi, C. R. *Science* **2000**, *287*, 2007.
9. Baskin, J. M.; Prescher, J. A.; Laughlin, S. T.; Agard, N. J.; Chang, P. V.; Miller, I. A.; Lo, A.; Codelli, J. A.; Bertozzi, C. R. *Proc. Natl. Acad. Sci. U.S.A.* **2007**, *104*, 16793.
10. Ning, X.; Guo, J.; Wolfert, M. A.; Boons, G. J. *Angew. Chem., Int. Ed.* **2008**, *120*, 2285.
11. Hong, V.; Presolski, S. I.; Ma, C.; Finn, M. G. *Angew. Chem., Int. Ed.* **2009**, *48*, 9879.
12. Hong, V.; Steinmetz, N. F.; Manchester, M.; Finn, M. G. *Bioconjug. Chem.* **2010**.
13. Neef, A. B.; Schultz, C. *Angew. Chem., Int. Ed.* **2009**, *48*, 1498.
14. Jao, C. Y.; Roth, M.; Welti, R.; Salic, A. *Proc. Natl. Acad. Sci. U.S.A.* **2009**, *106*, 15332.
15. Beatty, K. E.; Liu, J. C.; Xie, F.; Dieterich, D. C.; Schuman, E. M.; Wang, Q.; Tirrell, D. A. *Angew. Chem., Int. Ed.* **2006**, *45*, 7364.
16. Dieterich, D. C.; Link, A. J.; Graumann, J.; Tirrell, D. A.; Schuman, E. M. *Proc. Natl. Acad. Sci. U.S.A.* **2006**, *103*, 9482.
17. Weissleder, R.; Tung, C. H.; Mahmood, U.; Bogdanov, A. *Nat. Biotechnol.* **1999**, *17*, 375.
18. Jiang, T.; Olson, E. S.; Nguyen, Q. T.; Roy, M.; Jennings, P. A.; Tsien, R. Y. *Proc. Natl. Acad. Sci. U.S.A.* **2004**, *101*, 17867.
19. Blum, G.; Mullins, S. R.; Keren, K.; Fonovic, M.; Jedeszko, C.; Rice, M. J.; Sloane, B. F.; Bogyo, M. *Nat. Chem. Biol.* **2005**, *1*, 203.
20. Blum, G.; Degenfeld, G.; Merchant, M. J.; Blau, H. M.; Bogyo, M. *Nat. Chem. Biol.* **2007**, *3*, 668.
21. Yang, P. Y.; Liu, K.; Ngai, M. H.; Lear, M. J.; Wenk, M. R.; Yao, S. Q. *J. Am. Chem. Soc.* **2009**, *132*, 656.
22. DiDonato, D.; Brasaemle, D. L. *J. Histochem. Cytochem.* **2003**, *51*, 773.
23. Zimmermann, R.; Strauss, J. G.; Haemmerle, G. a. S. G.; Birner-Gruenberger, R.; Riederer, M.; Lass, A.; Neuberger, G.; Eisenhaber, F. a. H. A.; Zechner, R. *Science* **2004**, *306*, 1383.
24. Holm, C.; Fredrikson, G.; Cannon, B.; Belfrage, P. *Biosci. Rep.* **1987**, *7*, 897.
25. Karlsson, M.; Contreras, J. A.; Hellman, U.; Tornqvist, H.; Holm, C. *J. Biol. Chem.* **1997**, *272*, 27218.
26. Gilham, D.; Alam, M.; Gao, W. H.; Vance, D. E.; Lehner, R. *Mol. Biol. Cell* **2005**, *16*, 984.
27. Birner-Gruenberger, R.; Susani-Etzerodt, H.; Waldhuber, M.; Riesenhuber, G.; Schmidinger, H.; Rechberger, G.; Kollroser, M.; Strauss, J. G.; Lass, A. a. Z. R.; Haemmerle, G.; Zechner, R. a. H. A. *Mol. Cell. Proteomics* **2005**, *4*, 1710.
28. Zimmermann, R.; Strauss, J. G.; Haemmerle, G.; Schoiswohl, G.; Birner-Gruenberger, R.; Riederer, M.; Lass, A.; Neuberger, G.; Eisenhaber, F.; Hermetter, A.; Zechner, R. *Science* **2004**, *306*, 1383.
29. Heier, C.; Taschler, U.; Rengachari, S.; Oberer, M.; Wolinski, H.; Natter, K.; Kohlwein, S. D.; Leber, R.; Zimmermann, R. *Biochim. Biophys. Acta. Mol. Cell. Biol. Lipid* **2010**, *1801*, 1063.
30. Wang, H.; Wei, E.; Quiroga, A. D.; Sun, X.; Touret, N.; Lehner, R. *Mol. Biol. Cell* **2010**, *21*, 1991.
31. Lehner, R.; Verger, R. *Biochemistry* **1997**, *36*, 1861.
32. Rostovtsev, V. V.; Green, L. G.; Fokin, V. V.; Sharpless, K. B. *Angew. Chem., Int. Ed.* **2002**, *41*, 2596.
33. Abramoff, M. D.; Magelhaes, P. J.; Ram, S. J. *Biophot. Int.* **2004**, *11*, 36.
34. Lohse, P.; Chahrokh-Zadeh, S.; Lohse, P.; Seidel, D. *J. Lipid Res.* **1997**, *38*, 892.